



HAL
open science

The Evolving Role of Succinate in Tumor Metabolism: An 18 F-FDG–Based Study

Philippe Garrigue, Aurore Bodin-Hullin, Laure Balasse, Samantha Fernandez,
Wassim Essamet, Francoise Dignat-George, Karel Pacak, Benjamin Guillet,
David Taieb

► **To cite this version:**

Philippe Garrigue, Aurore Bodin-Hullin, Laure Balasse, Samantha Fernandez, Wassim Essamet, et al.. The Evolving Role of Succinate in Tumor Metabolism: An 18 F-FDG–Based Study: succinate and [18F]-FDG.. *Journal of Nuclear Medicine*, 2017, 58 (11), pp.1749-1755. 10.2967/jnumed.117.192674 . hal-01770170

HAL Id: hal-01770170

<https://amu.hal.science/hal-01770170>

Submitted on 24 Apr 2018

HAL is a multi-disciplinary open access archive for the deposit and dissemination of scientific research documents, whether they are published or not. The documents may come from teaching and research institutions in France or abroad, or from public or private research centers.

L'archive ouverte pluridisciplinaire **HAL**, est destinée au dépôt et à la diffusion de documents scientifiques de niveau recherche, publiés ou non, émanant des établissements d'enseignement et de recherche français ou étrangers, des laboratoires publics ou privés.

The evolving role of succinate in tumor metabolism: an [¹⁸F]-FDG-based study

Philippe Garrigue^{1,2,3}, Aurore Bodin-Hullin³, Laure Balasse^{1,2}, Samantha Fernandez²,
Wassim Essamet⁴, Françoise Dignat-George¹, Karel Pacak⁵, Benjamin Guillet^{1,2,3}, David Taïeb^{2,3}

¹Aix-Marseille Univ, Inserm, UMR-S 1076, Marseille, France.

²Aix-Marseille Univ, CERIMED, Marseille, France.

³Department of Nuclear Medicine, Aix-Marseille Univ, Marseille, France.

⁴APHM Timone Department of Neuropathology, Marseille, France

⁵Section on Medical Neuroendocrinology, *Eunice Kennedy Shriver* National Institute of Child Health & Human Development (NICHD), National Institutes of Health, Bethesda, Maryland, 20892 USA.

Abbreviated title: succinate and [¹⁸F]-FDG.

Key Terms: succinate, [¹⁸F]-FDG, succinate dehydrogenase, paraganglioma, tricarboxylic acid cycle

Total word count: 2984

Table(s): 0

Figure(s): 3

Suppl figure: 3

Corresponding author:

David Taïeb, MD, PhD

Department of Nuclear Medicine, La Timone University Hospital, European Center for Research
in Medical Imaging, Aix-Marseille University, 264 rue Saint-Pierre, 13385 Marseille, France,

Email: david.taieb@ap-hm.fr, Phone/FAX: +33 (0) 4-91-38-44-06.

Abstract

Objective. In recent years, inherited and acquired mutations in the TCA cycle enzymes have been reported in diverse cancers. Pheochromocytomas and paragangliomas (PPGLs) often exhibit dysregulation of glucose metabolism which is also driven by mutations in genes encoding the TCA cycle enzymes or by activation of hypoxia signaling. PPGLs associated with succinate dehydrogenase (*SDH*) deficiency are characterized by high ^{18}F -fluorodeoxyglucose (^{18}F -FDG) avidity. This association is currently only partially explained. Therefore, we hypothesized that accumulation of succinate due to the TCA cycle defect could be the major connecting hub between *SDH*-mutated tumors and ^{18}F -FDG uptake profile.

Design. To test whether succinate modifies the ^{18}F -FDG metabolic profile of tumors, we performed *in vitro* and *in vivo* (microPET/CT imaging and autoradiography) experiments in the presence of succinate, fumarate, and phosphate-buffered saline (PBS) in different cell models. As control, we also evaluated the impact of succinate on ^{18}F -fluorocholine uptake and retention.

GLUT1 immunohistochemistry was performed to assess whether ^{18}F -FDG uptake was correlated with GLUT1 staining.

Results. Intratumoral injection of succinate significantly increased ^{18}F -FDG uptake at 24 hours on microPET/CT imaging and autoradiography. No effect of succinate was observed on cancer cells *in vitro*, but interestingly, we found that succinate caused increased ^{18}F -FDG uptake by Human Umbilical Vein Endothelial Cells (HUVEC) in a concentration dependent manner. No significant effect was observed after intratumoral injection of fumarate or PBS. Succinate, fumarate, and PBS have no effect on cell viability, regardless of cell lineage. Intramuscular injection of succinate also significantly increases ^{18}F -FDG uptake by muscle when compared to

either PBS or fumarate, highlighting the effect of succinate on connective tissues. No difference was observed between PBS and succinate on [^{18}F]-fluorocholine uptake in the tumor and muscle and on hind limb blood flow. GLUT1 expression quantification did not significantly differ between the study groups.

Conclusions. The present study shows that succinate stimulates [^{18}F]-FDG uptake by endothelial cells, a finding which partially explains the [^{18}F]-FDG metabotype observed in tumors with SDH deficiency. Although this study is an [^{18}F]-FDG based approach, it provides an impetus to better characterize the determinants of [^{18}F]-FDG uptake in various tumors and their surrounding microenvironment with a special emphasis on the role of tumor specific oncometabolites.

Introduction

Succinate (succinic acid in blood pH) has only been considered for many decades as an intermediate metabolite of the tricarboxylic acid (TCA) cycle. During aerobic respiration, succinate is oxidized to fumarate, donating reducing equivalents. The reaction is catalyzed by succinate dehydrogenase (SDH), an enzyme complex located in the inner mitochondrial membrane that participates in both the TCA cycle and electron transport chain. SDH is composed of four nuclearly encoded subunits whose structure and genes have mostly been conserved through evolution. Hans Adolf Krebs team noticed some intermediates, including succinate, could accumulate in the interstitial space during liver ischemia (1). During ischemia, succinate can be produced by reduction of fumarate (a purine nucleotide cycle metabolite) via the reverse action of SDH. Succinate is then secondarily secreted from the cells into the blood stream (2). Many studies have shown that succinate has several functions beyond participating in the TCA cycle, of which some are mediated via a G protein-coupled succinate receptor (GPR91) (3). Through GPR91, succinate may have hormone-like actions in blood cells as well as fat, liver, heart, retina, and kidney tissues (4). For instance, in response to retinal ischemia, succinate plays an important role in the development of new blood vessels via GPR91 and subsequent modulation of VEGF release by retinal ganglion neurons (5).

Beyond cell functions described above, succinate and a few other TCA cycle intermediates were found to contribute to carcinogenesis (6). Recently, germline and somatic mutations in an additional three TCA cycle enzymes, fumarate hydratase (FH), malate dehydrogenase type 2 (MDH2), and isocitrate dehydrogenase (IDH) were identified in diverse cancers, which suggest metabolic alterations as the underlying hallmark of cancer. These mutations cause disruption of the TCA cycle and accumulation of TCA cycle intermediates,

ultimately altering various functions and the epigenome of cancer cells. These so-called oncometabolites were found to act as competitors of 2-oxoglutarate-dependent dioxygenases, which are involved in a broad spectrum of pathways such as hypoxic response, immune system dysfunction, and epigenetic reprogramming (7).

Pheochromocytomas and paragangliomas (PPGL) are tumors associated with TCA cycle defects (8). The most common cause of hereditary PPGL is SDH deficiency and accumulation of highly elevated levels of succinate. These tumors, unlike IDH-mutants tumors (9), are highly glucose avid (8). This metabolic pattern has been demonstrated by [¹⁸F]-fluorodeoxyglucose ([¹⁸F]-FDG) positron emission tomography (PET) imaging studies (10). This finding is attributed to activation of hypoxia signaling (8) and is in discordance with several experimental studies that have failed to identify increased glycolysis (11-15). Interestingly, neuroblastoma cell lines (a neural-crest tumor model similar to PPGL) with *SDHB* mutations were even found to have a paradoxical decrease in glucose uptake compared to wild-type cells, despite an increased growth rate and invasiveness (16). These effects were even more pronounced in the presence of human fibroblasts in co-culture experiments, indicating a possible metabolic cooperation between stroma and cancer cells (17). Primary human fibroblasts exhibit an increased glucose uptake when they are co-cultured with wild-type cells, and an even greater uptake when co-cultured with *SDHB*-silenced neuroblastoma cell lines. Several studies have shown that yeast with *sdh* Δ mutations may aberrantly efflux succinate from the mitochondria (18-20), and are therefore succinate is likely to act as an extracellular ligand. This efflux of succinate is also presumed in humans due to *SDH*-related PPGL patients have a higher value of plasma succinate-to-fumarate ratio compared to apparently sporadic and Neurofibromatosis type 1 (*NF1*) patients (21). Therefore, we hypothesized that succinate could be the connecting hub between *SDH* deficiency and tumor [¹⁸F]-FDG uptake profile via paracrine action on stroma cells.

Materials and Methods

Cells

Human umbilical vascular endothelial cells (HUVECs) are commonly used as a laboratory model system for studying the pathophysiology of endothelial cells (22) and tumor-stroma interactions (23). HUVECs were cultured in T175 plates in Endothelial Growth Medium-2 (EGM2, Lonza) supplemented with 10% decompemented fetal calf serum (FCS) at 37°C under 5% carbon dioxide (CO₂).

HT-29 is a human colorectal adenocarcinoma-derived cell line (obtained from a primary tumor). These cells were chosen because they have been fully characterized from an oncogenetic, metabolomics, and functional imaging standpoint. They are characterized by an activation of the mitogen-activated protein kinase pathway due to *BRAF* mutations (24), absence of succinate accumulation (25), and a moderate avidity for [¹⁸F]-FDG (26, 27). HT-29 cells were cultured in T175 plates in Dulbecco's Modified Eagle Medium (DMEM, Lonza) supplemented with 10% FCS at 37°C under 5% CO₂.

Primary human cardiac fibroblasts (HCF, PromoCell) were cultured in T175 plates in Fibroblast Growth Medium 3 (PromoCell) supplemented with 10% FCS at 37°C under 5% CO₂.

***In vitro* [¹⁸F]-FDG uptake by endothelial, tumor cells, and fibroblasts**

HT-29 cells, HUVECs, and primary human cardiac fibroblasts were transferred to 6-well flasks and pretreated for 24 hours with 0.01, 0.1, 1.0, or 10 nmol of succinate (Sigma-Aldrich) or fumarate (Sigma-Aldrich) per μL of culture medium. Fumarate or succinate solutions were prepared at 1 mmol/L, pH 7.4, in PBS. HT-29 cells allowed us to overcome the potential local

self-secretion of succinate by tumor cells that could prevaricate any exogenous succinate impact on [^{18}F]-FDG tissue uptake. Phosphate Buffer Saline (PBS) was used as a control. PBS was used as control. Each condition was repeated in triplicate. [^{18}F]-FDG was added (2 MBq/well) for 20 min, then the cells were washed three times with PBS, lysed with NaOH 0.2 M, and counted on COBRA-2 Auto gamma-counter (Packard). Counting results were corrected by physical decay ^{18}F and expressed as mean normalized [^{18}F]-FDG uptake.

***In vitro* evaluation of cell viability**

Cell viability was assessed by counting with Trypan blue on KOVA slides after a 24 hour incubation with 0.01 nmol/ μL or 10 nmol/ μL of fumarate or succinate, and then compared to PBS treatment. Counting results were expressed as mean normalized number of viable cells.

Mice

All procedures using animals were approved by the Institution's Animal Care and Use Committee (CE14, Aix-Marseille Université) and were conducted according to the EU Directive 2010/63/EU and the recommendations of the Helsinki Declaration. Six-week-old BALB/c mice ($n=12$) and Hsd:AthymicNude-Foxn1 nu mice ($n=15$) were purchased from Envigo. Animals were housed in enriched cages, placed in a temperature-and hygrometry-controlled room with daily monitoring, and fed with water and a commercial diet *ad libitum*.

Xenograft model

HT-29 cells (10^7) were trypsinized and re-suspended in 500 μ L of complete medium (Dulbecco's Modified Eagle Medium, 10% fetal calf serum, 100 U/mL penicillin, and 100 μ L Matrigel Basement Membrane Matrix High Concentration (Corning). Animals were then allowed to rest for 2 weeks. A first group of 3 Hsd:AthymicNude-Fox1nu mice was subcutaneously injected with 10^6 HT-29 cells/100 μ L on the right and left shoulders and on the right flank. A second group of 6 Hsd:AthymicNude-Fox1nu mice was subcutaneously injected with 10^6 HT-29 cells/100 μ L on the right shoulder with 10^6 HT-29 cells. A third group of 6 Hsd:AthymicNude-Fox1nu mice was subcutaneously injected the same way with 10^6 HT-29 cells/100 μ L on the right shoulder with 10^6 HT-29 cells.

***In vivo* [18 F]-FDG uptake following intratumoral injection of succinate**

Fourteen days after tumor engraftment, the xenografted mice from the first group were injected with 10 μ L of a 1 nmol/ μ L succinate solution in the right shoulder tumor with 10 μ L of a 1 nmol/ μ L fumarate solution in the left shoulder tumor, and with 10 μ L PBS in the right hind limb tumor every 6 hours for 24 hours under 1.5% isoflurane anesthesia ($n=3$). [18 F]-FDG injection (5-10 MBq/50 μ L, i.p.) was performed 3 hours after the last succinate injection.

PET images were acquired 40 min after injection on a Mediso NanoPET/CT under 1.5% isoflurane anesthesia. ROI quantification was performed on reconstructed PET/CT images, corrected by a tumor volume and pondered by animal weight.

At the end of the procedure, animals were euthanized with a lethal dose of pentobarbital, and the tumors were then explanted, stored in PFA4%, sliced, and directly exposed for 30 seconds to medium-sensitive phosphorimaging plates. Signals were analyzed by densitometry using Cyclone Plus® (Perkin-Elmer). Image analysis and quantifications were performed on

OptiQuant™ 5.0 software (Perkin-Elmer), results were expressed in digital light units per mm² (DLU/mm²) as mean \pm s_d.

***In vivo* dynamic [¹⁸F]-FDG and [¹⁸F]-fluorocholine uptake following intratumoral injection of succinate**

Fourteen days after tumor engraftment, the xenografted mice from the second group were injected with a 1 nmol/ μ L succinate solution or with PBS (10 μ L in the tumor, $n=3$ per condition) every 6 hours for 24 hours under 1.5% isoflurane anesthesia. [¹⁸F]-FDG injection (5-10 MBq/50 μ L, i.v.) was performed 3 hours after the last succinate injection. The xenografted mice from the third group were injected with a 1 nmol/ μ L succinate solution or with PBS (10 μ L in the tumor, $n=3$ per condition), every 6 hours for 24 hours under 1.5% isoflurane anesthesia. [¹⁸F]-fluorocholine injection (5-10 MBq/50 μ L, i.v.) was performed 3 hours after the last succinate injection. PET images were acquired beginning with the injection on a Mediso NanoPET/CT camera under 1.5% isoflurane anesthesia. PET images were reconstructed in dynamic mode with 10 frames of 1 minute, then 6 frames of 5 minutes followed by one 20-minutes frame. ROI quantification was performed on PET/CT images, corrected by a tumor volume.

***In vivo* dynamic [¹⁸F]-FDG and [¹⁸F]-fluorocholine uptake following intramuscular injections of succinate**

Twelve BALB/c mice were injected in the right *quadriceps femoris* muscle with succinate (10 μ L from a 1 nmol/ μ L solution) and in the left *quadriceps femoris* muscle with fumarate (10 μ L

from a 1 nmol/ μ L solution, “Fumarate/Succinate group”, $n=6$) or with PBS (“PBS/Succinate group”, $n=6$).

$[^{18}\text{F}]$ -FDG and $[^{18}\text{F}]$ -fluorocholine injections (5-10 MBq/50 μ L, i.v.) were performed on different groups 3 hours after the last succinate injection. PET images were acquired beginning with the injection on a Mediso NanoPET/CT camera under 1.5% isoflurane anesthesia. PET images were reconstructed in dynamic mode with 10 frames of 1 minutes, 6 frames of 5 minutes followed by one 20-minutes frame.

LASER-Doppler perfusion imaging (Perimed) was used to assess hind limb blood flow as previously described (28), right after the $[^{18}\text{F}]$ -FDG acquisition ($n=3$ per condition). Results were expressed as a ratio of succinate-treated limb to PBS- or fumarate-treated limb blood flow.

Immunohistochemistry

To assess whether the increased uptake was due to GLUT1 overexpression after succinate treatment, GLUT1 immunohistochemistry (GLUT-1, Rabbit Polyclonal Antibody, Thermo Scientific, RB-9052-P, dilution 1:200) was performed on HT-29 tumors and HUVECs treated with succinate, fumarate, or PBS. The immunoreactivity of GLUT1 was visually scored by a pathologist blinded to the study groups.

Statistics

Comparison of *in vitro* cellular uptake and cell viability were analyzed by 1-way ANOVA with *post-hoc* Bonferroni test. *In vivo* uptake of $[^{18}\text{F}]$ -FDG and $[^{18}\text{F}]$ -fluorocholine in muscles

and tumors and LASER-Doppler data were compared by two-tailed Mann-Whitney test. A P value of <0.05 indicated statistical significance.

Results

Succinate increases tumor [^{18}F]-FDG uptake and retention *in vivo*

To test whether succinate modifies the [^{18}F]-FDG metabolic pattern profile of tumors, we performed intratumoral injection of succinate in xenografts tumors. As a control, we also evaluated the effects when PBS and fumarate were injected. Tumor uptake was analyzed by microPET/CT imaging and autoradiography. Intratumoral injections of succinate significantly increased [^{18}F]-FDG uptake at 24 hours on microPET/CT ($P=0.0014$, $n=3$, **Fig. 1A**, **Suppl Fig 1**) and autoradiography ($P=0.0124$, $n=3$, **Fig. 1B**). Autoradiography resolution did not allow us to discriminate the effects of succinate in the different compartments *in vivo*. To test whether tracer uptake was linked to glucose metabolism and not related to increased blood flow or increased capillary permeability induced by succinate, we performed head-to-head comparison between [^{18}F]-FDG and [^{18}F]-Fluorocholine on dynamic $\mu\text{PET/CT}$. Intratumoral injections of succinate induced a significant increase in [^{18}F]-FDG uptake by tumors compared to the animals treated with PBS ($P<0.0096$, $n=3$, **Fig. 1C**) but no significant change in [^{18}F]-fluorocholine uptake was observed in both groups ($P=0.6088$, $n=3$, **Fig. 1D**).

Succinate increases [^{18}F]-FDG uptake by endothelial cells, but not in tumor cells or

fibroblasts *in vitro*

We next sought to obtain information on whether tumor and/or stroma cells could be responsible for our observed metabolic changes. Tumors, endothelial cells, and fibroblasts were treated with varying concentrations of succinate, as well as PBS and fumarate as controls. To test whether succinate could produce metabolic changes independently of cell density, we analyzed both [¹⁸F]-FDG uptake and cell viability. We found that both the presence of succinate and its concentration significantly influenced [¹⁸F]-FDG uptake by endothelial cells ($P=0.0023$, $n=3$). Compared to fumarate, succinate significantly increased [¹⁸F]-FDG uptake by HUVECs at concentrations of 0.1 ($P=0.0125$, $n=3$), 1.0 ($P=0.0028$, $n=3$), and 10 nmol/ μ L ($P=0.0008$, $n=3$). No significant effect was observed at 0.01 nmol/ μ L of succinate (**Fig. 2**). Succinate slightly, but not significantly, decreased [¹⁸F]-FDG uptake by HT-29 cells and fibroblasts. No matter the cell lineage, total number of live cells was not significantly affected by the presence of succinate when compared to fumarate and PBS.

Succinate increases *in vivo* [¹⁸F]-FDG uptake and retention by connective tissue

To test whether a modification in uptake pattern of connective tissue could produce the changes on PET imaging, we evaluated the effects of intramuscular administration of succinate in mice. Intramuscular injections of succinate induced a significant increase in [¹⁸F]-FDG uptake by muscle compared to the contralateral muscle injected with either PBS ($P=0.0162$, $n=3$) or fumarate ($P=0.0458$, $n=3$, **Fig. 3A**). Intramuscular injection of succinate did not affect [¹⁸F]-fluorocholeline uptake compared to the contralateral muscle injected with either PBS ($P=0.6173$, $n=3$) or fumarate ($P=0.92303$, $n=3$, **Fig. 3B**). Finally, no difference on hind limb blood flow was

observed on LASER-Doppler ($P=1.000$, $n=3$ and $P=0.7500$, $n=3$ respectively, **Fig. 3C**).

GLUT1 Immunohistochemistry

GLUT1 expression quantification did not significantly differ between study groups in HUVECs or HT-29 tumors (in both epithelial and stromal compartments) (**Suppl Fig 2 and 3**).

Discussion

It is now evident that succinate should not only be viewed as a metabolite donor in the TCA cycle, but also as a signaling molecule with hormone-like functions, which could play a vital role during various pathophysiological conditions such as ischemia (4) and inflammation (29). The identification of cancer-associated mutations in the TCA cycle enzymes has also highlighted the prevailing notion that aberrant metabolic function can contribute to carcinogenesis via a broad spectrum of pathways such as hypoxic, inflammation and immune system responses, and epigenetic reprogramming (30, 31). Succinate has been shown to stabilize HIF- via inhibition of prolyl hydroxylases in the cytosol, suggesting a mechanistic link between *SDHx* mutations, high tumor vascularity, and [¹⁸F]-FDG uptake profile in absence of *VHL* mutations (12, 32). Although this hypothesis is appealing, it should probably be applied to all tumors. Furthermore, the metabolic impact of a malfunctioning TCA is partially compensated by the activation of several alternative pathways that can provide metabolites that can enter the TCA at various checkpoints (15, 33).

It is well understood that the quantification of tumor [¹⁸F]-FDG uptake by PET imaging can be hampered by the contribution of the metabolized [¹⁸F]-FDG fraction located within stroma cells. Additionally, the un-metabolized component of [¹⁸F]-FDG (in the blood within a tumor, in the intercellular spaces, and within the tumor and stroma cells themselves) can also be far from negligible in certain circumstances. During the past 10 years, studies have shown that *SDHx*-PPGLs exhibit highly elevated [¹⁸F]-FDG uptake. Recently, we have shown in a small series that high standardized uptake value (SUV) values can be observed in PPGL despite relative low k_3 values (the rate constant for [¹⁸F]-FDG phosphorylation) compared to malignancies which exhibit high k_3 values (34). This finding suggested that increased [¹⁸F]-FDG uptake cannot be

solely explained by intense tumor cell metabolism and could potentially involve the stroma cells.

The present study shows a new hypothesis based on the effect of succinate on [^{18}F]-FDG uptake by endothelial cells, expanding its repertoire of extracellular functions. This could partially explain the [^{18}F]-FDG uptake pattern observed in PPGLs, which are highly vascularized tumors. We also demonstrated that succinate-induced ^{18}F -FDG uptake was not due to increased blood flow or increased capillary permeability since this phenomenon was not observed after injection of [^{18}F]-Fluorocholine and no increased blood flow was observed on LASER-Doppler .

The concentrations used throughout this study (0 to 10 nmol/ μL) were previously identified as appropriate by metabolomics studies which did not distinguish intra from extracellular succinate components. Many studies have shown that *SDH* mutated tumors contain enormous levels of succinate (35-38) that could even be detected by in *vivo* MR spectroscopy (39, 40). It is probable that large amounts of succinate are effluxed by the mutated cells. Analyses of compartmentalized levels of TCA cycle metabolites have revealed that yeast with *sdh Δ* mutations may aberrantly efflux succinate from the mitochondria to the cytosol (18). Other studies have even reported that succinate could be excreted into the medium during cultivation of yeast *sdh Δ* mutants (19, 20). It has been speculated that this retrograde pathway may prevent the potential detrimental effects of succinate excess on non-mitochondrial processes (41). Succinate can migrate through the mitochondrial and plasma membrane via different transport systems such as a succinate-fumarate transporter in the inner mitochondrial membrane, porins in the outer mitochondrial membrane, and a sodium-independent anion exchanger in the plasma membrane.

The present study shows that endothelial cells may play an important role in [^{18}F]-FDG uptake, and perhaps in some tumors, they significantly contribute to a final [^{18}F]-FDG PET image. This finding will provide incentive to better characterize the molecular mechanisms involved in increased [^{18}F]-FDG uptake in various tumors, including PPGLs TCA cycle defects.

Unfortunately, due to the lack of a well-characterized human PPGL cell line, further validation is not yet possible. The present results also suggest that tumor microenvironment plays an extraordinary role in supplying energy and metabolic fuel for a tumor cell (42, 43). Notably, the increased glucose uptake in endothelial cells is not due to increased GLUT1 expression. However, this could be due to the involvement of other glucose transporters and/or increased activity of intracellular hexokinases (44). Finally, it would be interesting to use GPR91 antagonists or nitric oxide (NO) signaling modulation to study the signaling pathway involved in succinate-induced glucose uptake by endothelial cells (45, 46). If so, this concept could propose a novel therapeutic approach on starving PPGL via inhibition of GPR91 or NO signaling.

References

1. Brosnan JT, Krebs HA, Williamson DH. Effects of ischaemia on metabolite concentrations in rat liver. *Biochem J*. Mar 1970;117(1):91-96.
2. Chouchani ET, Pell VR, Gaude E, et al. Ischaemic accumulation of succinate controls reperfusion injury through mitochondrial ROS. *Nature*. Nov 20 2014;515(7527):431-435.
3. He W, Miao FJ, Lin DC, et al. Citric acid cycle intermediates as ligands for orphan G-protein-coupled receptors. *Nature*. May 13 2004;429(6988):188-193.
4. de Castro Fonseca M, Aguiar CJ, da Rocha Franco JA, Gingold RN, Leite MF. GPR91: expanding the frontiers of Krebs cycle intermediates. *Cell Commun Signal*. Jan 12 2016;14:3.
5. Sapieha P, Sirinyan M, Hamel D, et al. The succinate receptor GPR91 in neurons has a major role in retinal angiogenesis. *Nat Med*. Oct 2008;14(10):1067-1076.
6. Hanahan D, Weinberg RA. Hallmarks of cancer: the next generation. *Cell*. Mar 4 2011;144(5):646-674.
7. Letouze E, Martinelli C, Lorient C, et al. SDH Mutations Establish a Hypermethylator Phenotype in Paraganglioma. *Cancer cell*. Jun 10 2013;23(6):739-752.

8. Jochmanova I, Pacak K. Pheochromocytoma: The First Metabolic Endocrine Cancer. *Clin Cancer Res.* Oct 15 2016;22(20):5001-5011.
9. Metellus P, Colin C, Taieb D, et al. IDH mutation status impact on in vivo hypoxia biomarkers expression: new insights from a clinical, nuclear imaging and immunohistochemical study in 33 glioma patients. *J Neurooncol.* Dec 2011;105(3):591-600.
10. Taieb D, Timmers HJ, Shulkin BL, Pacak K. Renaissance of (18)F-FDG positron emission tomography in the imaging of pheochromocytoma/paraganglioma. *J Clin Endocrinol Metab.* Jul 2014;99(7):2337-2339.
11. Burnichon N, Vescovo L, Amar L, et al. Integrative genomic analysis reveals somatic mutations in pheochromocytoma and paraganglioma. *Hum Mol Genet.* Oct 15 2011;20(20):3974-3985.
12. Favier J, Briere JJ, Burnichon N, et al. The Warburg effect is genetically determined in inherited pheochromocytomas. *PLoS One.* 2009;4(9):e7094.
13. Lopez-Jimenez E, Gomez-Lopez G, Leandro-Garcia LJ, et al. Research Resource: Transcriptional Profiling Reveals Different Pseudohypoxic Signatures in SDHB and VHL-Related Pheochromocytomas. *Mol Endocrinol.* Dec 2010;24(12):2382-2391.

14. Pollard PJ, El-Bahrawy M, Poulson R, et al. Expression of HIF-1alpha, HIF-2alpha (EPAS1), and their target genes in paraganglioma and pheochromocytoma with VHL and SDH mutations. *J Clin Endocrinol Metab.* Nov 2006;91(11):4593-4598.
15. Lussey-Lepoutre C, Hollinshead KE, Ludwig C, et al. Loss of succinate dehydrogenase activity results in dependency on pyruvate carboxylation for cellular anabolism. *Nat Commun.* 2015;6:8784.
16. Rapizzi E, Ercolino T, Fucci R, et al. Succinate dehydrogenase subunit B mutations modify human neuroblastoma cell metabolism and proliferation. *Horm Cancer.* Jun 2014;5(3):174-184.
17. Rapizzi E, Fucci R, Giannoni E, et al. Role of microenvironment on neuroblastoma SK-N-AS SDHB-silenced cell metabolism and function. *Endocr Relat Cancer.* Jun 2015;22(3):409-417.
18. Lin AP, Anderson SL, Minard KI, McAlister-Henn L. Effects of excess succinate and retrograde control of metabolite accumulation in yeast tricarboxylic cycle mutants. *J Biol Chem.* Sep 30 2011;286(39):33737-33746.
19. Szeto SS, Reinke SN, Sykes BD, Lemire BD. Ubiquinone-binding site mutations in the *Saccharomyces cerevisiae* succinate dehydrogenase generate superoxide and lead to the accumulation of succinate. *J Biol Chem.* Sep 14 2007;282(37):27518-27526.

20. Szeto SS, Reinke SN, Sykes BD, Lemire BD. Mutations in the *Saccharomyces cerevisiae* succinate dehydrogenase result in distinct metabolic phenotypes revealed through (1)H NMR-based metabolic footprinting. *J Proteome Res.* Dec 03 2010;9(12):6729-6739.
21. Lendvai N, Pawlosky R, Bullova P, et al. Succinate-to-fumarate ratio as a new metabolic marker to detect the presence of SDHB/D-related paraganglioma: initial experimental and ex vivo findings. *Endocrinology.* Jan 2014;155(1):27-32.
22. Park HJ, Zhang Y, Georgescu SP, Johnson KL, Kong D, Galper JB. Human umbilical vein endothelial cells and human dermal microvascular endothelial cells offer new insights into the relationship between lipid metabolism and angiogenesis. *Stem Cell Rev.* 2006;2(2):93-102.
23. Correa de Sampaio P, Auslaender D, Krubasik D, et al. A heterogeneous in vitro three dimensional model of tumour-stroma interactions regulating sprouting angiogenesis. *PLoS One.* 2012;7(2):e30753.
24. Ahmed D, Eide PW, Eilertsen IA, et al. Epigenetic and genetic features of 24 colon cancer cell lines. *Oncogenesis.* Sep 16 2013;2:e71.
25. Haraguchi T, Kayashima T, Okazaki Y, et al. Cecal succinate elevated by some dietary polyphenols may inhibit colon cancer cell proliferation and angiogenesis. *J Agric Food Chem.* Jun 18 2014;62(24):5589-5594.

26. Burt BM, Humm JL, Kooby DA, et al. Using positron emission tomography with [(18)F]FDG to predict tumor behavior in experimental colorectal cancer. *Neoplasia*. May-Jun 2001;3(3):189-195.
27. Li XF, Ma Y, Sun X, Humm JL, Ling CC, O'Donoghue JA. High 18F-FDG uptake in microscopic peritoneal tumors requires physiologic hypoxia. *J Nucl Med*. Apr 2010;51(4):632-638.
28. Bennis Y, Sarlon-Bartoli G, Guillet B, et al. Priming of late endothelial progenitor cells with erythropoietin before transplantation requires the CD131 receptor subunit and enhances their angiogenic potential. *J Thromb Haemost*. Sep 2012;10(9):1914-1928.
29. Tannahill GM, Curtis AM, Adamik J, et al. Succinate is an inflammatory signal that induces IL-1beta through HIF-1alpha. *Nature*. Apr 11 2013;496(7444):238-242.
30. Ghaffari P, Mardinoglu A, Nielsen J. Cancer Metabolism: A Modeling Perspective. *Front Physiol*. 2015;6:382.
31. Delgoffe GM, Powell JD. Feeding an army: The metabolism of T cells in activation, anergy, and exhaustion. *Mol Immunol*. Dec 2015;68(2 Pt C):492-496.
32. Selak MA, Armour SM, MacKenzie ED, et al. Succinate links TCA cycle dysfunction to oncogenesis by inhibiting HIF-alpha prolyl hydroxylase. *Cancer Cell*. Jan 2005;7(1):77-85.

33. Zielinski LP, Smith AC, Smith AG, Robinson AJ. Metabolic flexibility of mitochondrial respiratory chain disorders predicted by computer modelling. *Mitochondrion*. Nov 2016;31:45-55.
34. Barbolosi D, Hapdey S, Battini S, et al. Determination of the unmetabolised F-FDG fraction by using an extension of simplified kinetic analysis method: clinical evaluation in paragangliomas. *Med Biol Eng Comput*. Jun 5 2015.
35. Imperiale A, Moussallieh FM, Roche P, et al. Metabolome profiling by HRMAS NMR spectroscopy of pheochromocytomas and paragangliomas detects SDH deficiency: clinical and pathophysiological implications. *Neoplasia*. Jan 2015;17(1):55-65.
36. Imperiale A, Moussallieh FM, Sebag F, et al. A new specific succinate-glutamate metabolomic hallmark in SDHx-related paragangliomas. *PloS one*. 2013;8(11):e80539.
37. Richter S, Peitzsch M, Rapizzi E, et al. Krebs cycle metabolite profiling for identification and stratification of pheochromocytomas/paragangliomas due to succinate dehydrogenase deficiency. *J Clin Endocrinol Metab*. Oct 2014;99(10):3903-3911.
38. Rao JU, Engelke UF, Sweep FC, et al. Genotype-specific differences in the tumor metabolite profile of pheochromocytoma and paraganglioma using untargeted and targeted metabolomics. *J Clin Endocrinol Metab*. Feb 2015;100(2):E214-222.

39. Varoquaux A, Le Fur Y, Imperiale A, et al. Magnetic resonance spectroscopy of paragangliomas: new insights into in vivo metabolomics. *Endocr Relat Cancer*. Jun 26 2015.
40. Lussey-Lepoutre C, Bellucci A, Morin A, et al. In Vivo Detection of Succinate by Magnetic Resonance Spectroscopy as a Hallmark of SDHx Mutations in Paraganglioma. *Clin Cancer Res*. Mar 1 2016;22(5):1120-1129.
41. Pollard PJ, Briere JJ, Alam NA, et al. Accumulation of Krebs cycle intermediates and over-expression of HIF1alpha in tumours which result from germline FH and SDH mutations. *Hum Mol Genet*. Aug 1 2005;14(15):2231-2239.
42. Gravel SP, Avizonis D, St-Pierre J. Metabolomics Analyses of Cancer Cells in Controlled Microenvironments. *Methods Mol Biol*. 2016;1458:273-290.
43. Carito V, Bonuccelli G, Martinez-Outschoorn UE, et al. Metabolic remodeling of the tumor microenvironment: migration stimulating factor (MSF) reprograms myofibroblasts toward lactate production, fueling anabolic tumor growth. *Cell Cycle*. Sep 15 2012;11(18):3403-3414.
44. Tumova S, Kerimi A, Porter KE, Williamson G. Transendothelial glucose transport is not restricted by extracellular hyperglycaemia. *Vascul Pharmacol*. Dec 2016;87:219-229.
45. Leite LN, Gonzaga NA, Simplicio JA, et al. Pharmacological characterization of the mechanisms underlying the vascular effects of succinate. *Eur J Pharmacol*. Oct 15 2016;789:334-343.

46. Paik JY, Lee KH, Ko BH, Choe YS, Choi Y, Kim BT. Nitric oxide stimulates ¹⁸F-FDG uptake in human endothelial cells through increased hexokinase activity and GLUT1 expression. *J Nucl Med.* Feb 2005;46(2):365-370.

Legends

Figure 1

A: (top) Representative PET/CT images of HT-29 tumor-bearing mice ($n=3$) 40 minutes after [^{18}F]-FDG injection (5-10 MBq/50 μL , i.p.) and 27 hours after the first 10 μL -intratumoral injection of 1 mM succinate (right shoulder, red arrow), 1 mM fumarate (left shoulder, green arrow), or PBS (right hind limb, yellow arrow) every 6 hours for 24 hours. (bottom) Quantification from [^{18}F]-FDG microPET/CT in tumors. $**P<0.01$ (One-way ANOVA with Bonferroni post-hoc test, $n=3$ per condition).

B: (top) Representative autoradiographic images of HT-29 tumors extracted from mice right after the microPET/CT imaging (bottom). Quantification from tumor autoradiography. $*P<0.05$ (One-way ANOVA with Bonferroni post-hoc test, $n=3$ per condition).

C: (top) Representative microPET/CT images of mice hind limbs ($n=3$) 40 minutes after [^{18}F]-FDG injection (5-10 MBq/50 μL , i.v.) and 27 hours after the first succinate or PBS injection every 6 hours for 24 hours. Bottom graph shows corresponding quantifications expressed in % of the injected dose per gram of tissue over time, from dynamic microPET/CT reconstruction. $**P<0.01$ (Mann-Whitney test, $n=3$ per condition).

D: (top) Representative microPET/CT images 40 minutes after [^{18}F]-fluorocholine injection (5-7 MBq/50 μL , i.v.) and 27 hours after the first succinate or PBS injection every 6 hours for 24 hours. Bottom graph shows corresponding quantifications expressed in % of the injected dose

per gram of tissue over time, from dynamic microPET/CT reconstruction. (Mann-Whitney test, $n=3$ per condition).

Figure 2

Influence of succinate pretreatment on [^{18}F]-FDG uptake in HUVECs (A, top), in HT-29 cells (B, top) and in primary cardiac fibroblasts (C, top) after pretreatment for 24 hours with 0, 0.01, 0.1, 1.0, or 10 nmol of succinate per μL of culture medium. * $P<0.05$, ** $P<0.01$, *** $P<0.001$ (2-way ANOVA with Bonferroni post-hoc test, $n=3$ per condition).

Viability of HUVECs (A, bottom), HT-29 cells (B, bottom) and fibroblasts (C, bottom) by counting on KOVA slides with Trypan blue after a 24 hour incubation with 0.01 nmol/ μL or 10 nmol/ μL of fumarate or succinate, compared to PBS treatment (2-way ANOVA with Bonferroni post-hoc test, $n=3$ per condition).

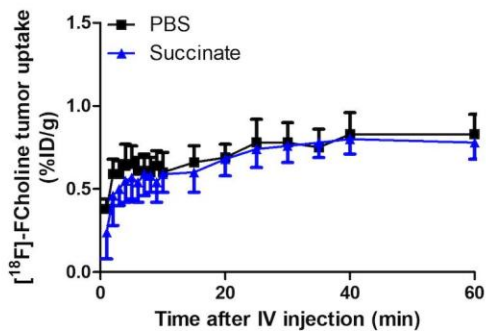
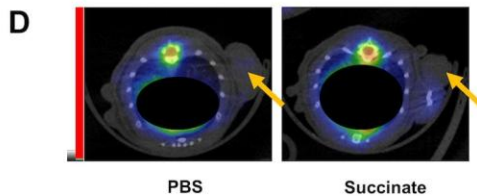
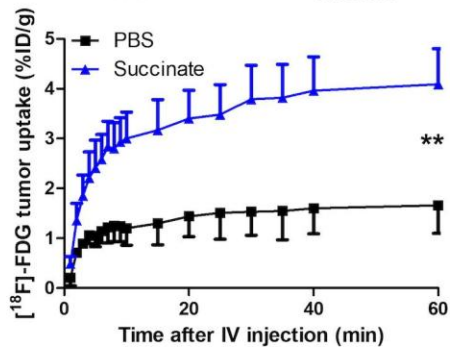
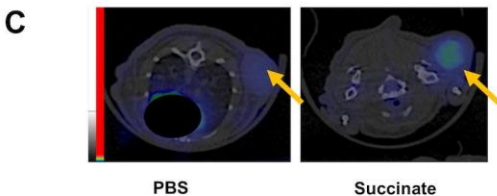
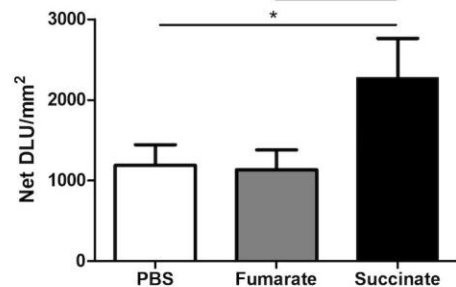
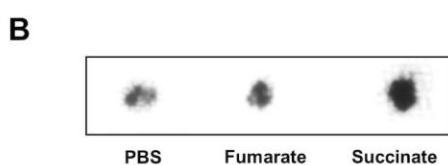
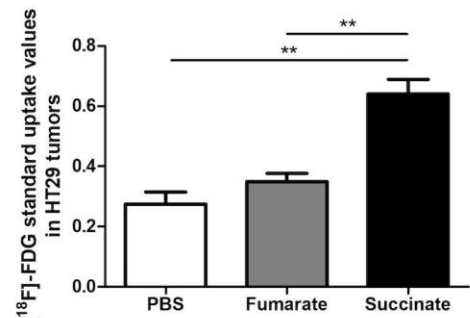
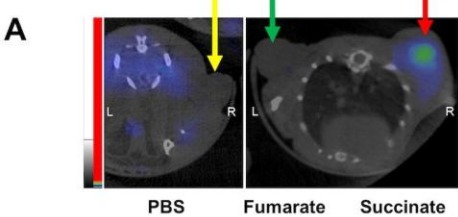
Figure 3

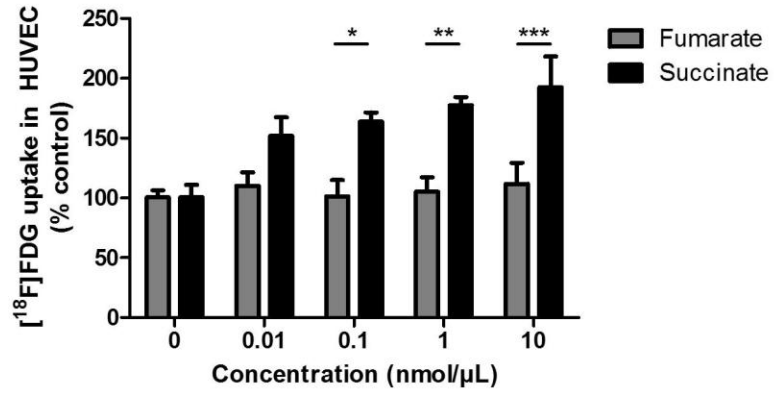
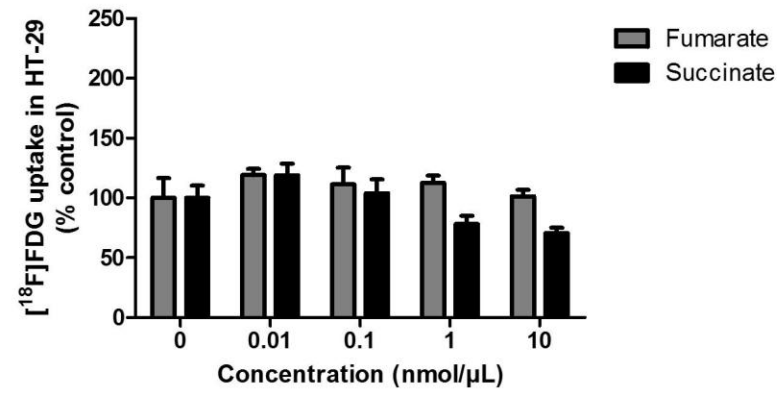
A: Representative microPET/CT images of mice hind limbs ($n=3$) 40 minutes after [^{18}F]-FDG injection (5-10 MBq/50 μL , i.v.) and 27 hours after the first succinate (right hind limb) or fumarate or PBS (left hind limb) injection every 6 hours for 24 hours. Bottom graph shows corresponding quantifications in each hind limb expressed in % of the injected dose per gram of tissue over time, from dynamic microPET/CT reconstruction. * $P<0.05$ (Mann-Whitney test, $n=3$ per condition).

B: Representative microPET/CT images of mice hind limbs ($n=3$) 40 minutes after [^{18}F]-fluorocholine injection (5-7 MBq/50 μL , i.v.) and 27 hours after the first succinate (right hind limb) or fumarate or PBS (left hind limb) injection every 6 hours for 24 hours. Bottom graph shows corresponding quantifications in each hind limb expressed in % of the injected dose per gram of tissue over time, from dynamic microPET/CT reconstruction. (Mann-Whitney test, $n=3$ per condition).

C: Representative LASER-Doppler perfusion images of mice hind limbs ($n=6$), right after [^{18}F]-FDG PET (28 hours after the first succinate (right hind limb) or fumarate or PBS (left hind limb) injection every 6 hours for 24 hours.

Bottom graphs show corresponding quantifications of the perfusion signal in each hind limb.



A**B****C**